

*IDA*

INSTITUTE FOR DEFENSE ANALYSES

**Measurement of Gradient Index Materials by  
Beam Deflection, Displacement, or Mode  
Conversion (Journal Version)**

Jeremy Teichman

March 2013

Approved for public release;  
distribution is unlimited.

IDA Paper NS P-4994

Log: H 13-001311

INSTITUTE FOR DEFENSE ANALYSES  
4850 Mark Center Drive  
Alexandria, Virginia 22311-1882



*The Institute for Defense Analyses is a non-profit corporation that operates three federally funded research and development centers to provide objective analyses of national security issues, particularly those requiring scientific and technical expertise, and conduct related research on other national challenges.*

#### About This Publication

This work was conducted by the Institute for Defense Analyses (IDA) under contract W91WAW-11-C-0003, Task DA-2-3226, "Manufacturable Gradient Index (GRIN) Optics," for the Defense Advanced Research Projects Agency (DARPA). The views, opinions, and findings should not be construed as representing the official position of either the Department of Defense or the sponsoring organization.

#### Copyright Notice

© 2013 Institute for Defense Analyses  
4850 Mark Center Drive, Alexandria, Virginia 22311-1882 • (703) 845-2000.

# Measurement of gradient index materials by beam deflection, displacement, or mode conversion

---

*Jeremy Teichman, Institute for Defense Analyses, March 9, 2013*

**Abstract:** *For media with heterogeneous index of refraction, rays follow curved paths. This paper describes methods exploiting knowledge of the relationship between refractive index distribution and ray paths to estimate the refractive index distribution based on laser beam deflection, displacement, and mode conversion on passage through the media. The work covers axial, radial (cylindrical), and spherical refractive index distributions.*

## 1. Introduction

---

Recent advances in manufacturing methods for gradient index optical components would benefit from accompanying non-destructive metrology techniques faster than current precision interferometric methods. Manufacturers require measurement of the spatially varying refractive index profiles in these components in order to evaluate parts and processes as well as to locate and orient the index distribution for cutting and forming. This paper describes techniques using geometric optics to reconstruct the refractive index distribution in a sample based on measurement of laser beam displacement, deflection, and to a lesser degree mode conversion after passing through samples with axial, radial (cylindrical), or spherical gradients of refractive index.

Ray paths confined to a plane, as occurs in a plane of refractive index symmetry, obey

$$\frac{ny''}{1+y'^2} = \frac{\partial n}{\partial x} y' - \frac{\partial n}{\partial y}, \quad (1)$$

where  $\vec{r}$  is the position of a point on the ray,  $n$  is the index of refraction, the ray path is defined by  $y = y(x)$ , and primes indicate differentiation with respect to  $x$  (e.g. [1]). For axial, radial, and spherical gradients of refractive index, Eq. 1 reduces to an ordinary

differential equation. Integration of the resulting equation results in a relationship between the refractive index distribution and the ray paths that can be exploited to estimate the refractive index distribution based on measurements of laser beams passing through the media. The methods presented here do not rely on measurement of the full path of the beams through the media; they utilize only the beam conditions at the entry and exit points measurable from outside the media. Beam position, direction, and mode shape are all considered. If, due to scatter in the media, the entire beam path can be observed and measured, the index all along the beam path relative to that at beam entry can be directly calculated using the local slope of the ray path.

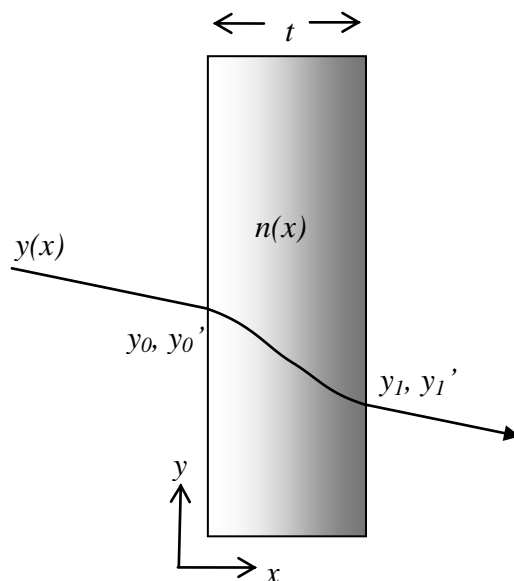
Due to similarities in symmetry, radial gradients behave like spherical gradients when viewed normal to the axis of symmetry and like axial gradients when viewed along the axis of symmetry. Therefore, the following three cases suffice to cover the three basic gradient structures: axial viewed normal to the gradient and parallel to the gradient and spherical. The methods are constructed using basic manufacturing shapes for optical blanks (slabs for the axial gradients, rods for the cylindrical gradients, and spheres for the spherical gradients); however, as long as the cut surface shape is known, the methods apply equally to finished components.

Previous work by others, beginning in 1893 with Weiner [2], includes examining index reconstruction

- by known ray-paths through the full span of a planar or arbitrary medium [3] [4];
- for planar wave-guides with fixed index faces [5];
- for thin-medium, small displacement, normal beam-incidence [6]; and
- for cylindrical fiber preforms [7].

## 2. Axial Gradient across a Slab

---



For this case, Eq. 1 reduces to

$$-\frac{y''}{y'(1+y'^2)} = \frac{1}{n} \frac{dn}{dx}, \quad (2)$$

which can be integrated to produce

$$\frac{1 + \frac{1}{y'^2}}{1 + \frac{1}{y_0'^2}} = \frac{n^2}{n_0^2}, \quad (3)$$

where  $n_0$  is the index of refraction on the entrance face and  $y_0'$  is the entrance slope. Eq. 3 indicates that the local slope of a ray path with given entrance conditions will depend only on the local index of refraction and the index and slope on the entry face. Eq. 4 is equivalent to a Snell's-law invariant along any ray,  $n^2 \sin^2 \theta = \text{constant}$ , where  $\theta$  is the angle between the ray and the  $x$ -axis and the surface normal in Snell's law has been replaced by the refractive index gradient, which is normal to the iso-indicial surfaces. Measurement of the exit slope would allow direct calculation of the index on the exit face. Further integration of Eq. 3 across the thickness of the slab yields

$$\Delta y \equiv y_1 - y_0 = \int_0^t \frac{dx}{\sqrt{\frac{n^2}{n_0^2} \left(1 + \frac{1}{y_0'^2}\right) - 1}}. \quad (4)$$

Because the angular deflection and vertical displacement of the beam will not depend on initial vertical position, the mode shape of a beam will be preserved through the slab, and no additional information can be obtained using beam mode shapes. The deflection of the beam  $y_1'(y_0')$  depends only on the exit index, not on the interior variation. Only the variation of displacement  $\Delta y$  with the entrance slope will provide information about the interior index profile.

Two basic approaches to the solution of Eq. 4 could be considered. Particularly in a manufacturing metrology setting where the element has a known target index profile, an iterative approach to solving a discrete version of Eq. 4 would probably be appropriate. In such an approach the postulated index distribution would be iteratively adjusted, starting with an initial guess given by the target profile to minimize the magnitude of the residual between the measured beam displacement and that predicted by the evaluation of the right-hand side of Eq. 4 using the postulated index distribution.

Alternatively, one could attempt to construct the profile directly. An analytic approach is possible using methods of integral equations under limiting assumptions about the profile. For instance, if the profile is assumed to be monotonic with position (so that  $n(x)$  can be inverted to  $x(n)$ ), the following transformation could be applied (without loss of generality assume  $n_1 > n_2$ )

$$\begin{aligned} \zeta &\equiv \frac{-n_0^2}{1 + y_0'^2} \\ \eta &\equiv n^2 - n_0^2 \\ f(\zeta) &\equiv \frac{\Delta y(y_0'(\zeta))}{\sqrt{\zeta + n_0^2}} = \int_0^t \frac{dx}{\sqrt{n^2(x) - \zeta - n_0^2}} \\ &= \int_0^{n_1^2 - n_0^2} \frac{g(\eta) d\eta}{\sqrt{\eta - \zeta}}, \end{aligned} \quad (5)$$

where

$$g(\eta) \equiv \frac{dx}{d\eta}.$$

$n(x)$  can be reconstructed if  $g(\eta)$  is known by inverting

$$x(n) = \int_0^n 2ng(n^2 - n_0^2) dn.$$

Eq. 5 theoretically has an analytic solution [8],

$$g(\eta) = \frac{-1}{\sqrt{8\pi}\Gamma^2\left(\frac{3}{4}\right)\eta^{\frac{1}{4}}}\frac{d}{d\eta}\left[\int_{\eta}^{n_1^2-n_0^2}\frac{dv}{\sqrt{v-\eta}}\int_0^v\frac{f(\zeta)d\zeta}{\zeta^{\frac{1}{4}}(v-\zeta)^{\frac{1}{4}}}\right]. \quad (6)$$

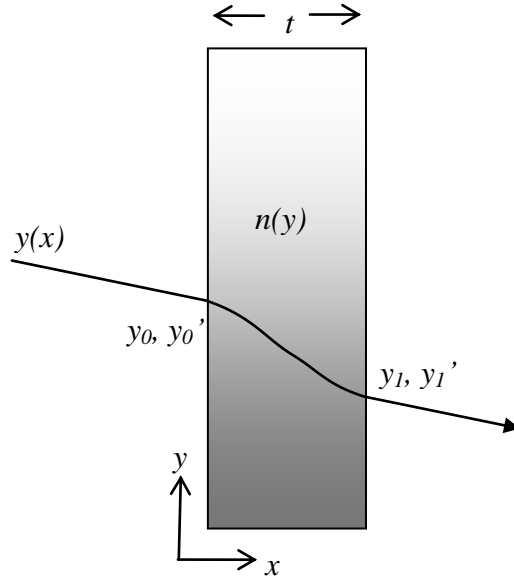
Unfortunately, note that  $\zeta < 0$  and the innermost integral must take positive values from 0 to  $n_1^2 - n_0^2$ . Alternatively, for inverting a finite set of measurements ( $m = 1 \cdots M$ ), a piecewise construction of the index using any explicitly integrable functional form for the segments would yield the set of  $M$  nonlinear equations

$$f(\zeta_m) = \sum_{k=1}^K \int_{\frac{(k-1)t}{K}}^{\frac{kt}{K}} \frac{dx}{\sqrt{n_k^2(x) - n_0^2 - \zeta_m}}. \quad (7)$$

By choosing the number of segments such that the total number of unknowns is equal to or less than the number of measurements, the system could be solved using standard methods. This second method closely resembles the first, although, in the first method, numerical integration and any reasonably parameterized form of index profile could be used. With the first method, an index profile form with more parameters than the number of measurements would be vulnerable non-unique solutions.

### 3. Axial Gradient along a Slab or Cross-section of a Radial Gradient

---



For this case, Eq. 1 reduces to

$$ny'' = \frac{dn}{dy}(1 + y'^2). \quad (8)$$

Examination of Eq. 8 reveals that the ray path is dependent only on the local logarithmic derivative of the index of refraction. A boundary condition on the index must be known to solve for the absolute index of refraction. Integration of Eq. 8 yields

$$\frac{1 + y'^2}{1 + y_0'^2} = \frac{n^2}{n_0^2}. \quad (9)$$

Therefore, measurement of the entrance and exit slopes of the beam directly gives the ratio of indices at the beam entry and exit points. Measurement of the slope could, for example, be done with two partly scattering screens at different known distances from the beam exit. Eq. 9 expresses the same invariant as Eq. 3 in a rotated reference frame where the iso-indicial surfaces are now normal to the  $y$ -axis. In principle, Eq. 9 with data from a sweep over the full height of the slab would enable what amounts to numerical integration of the index (assuming as a boundary condition a region of known index).

Rearranging Eq. 9 and integrating yields

$$t = \int_{y_0}^{y_1} \frac{dy}{\sqrt{(1 + y_0'^2) \frac{n^2}{n_0^2} - 1}}. \quad (10)$$

Measurement of the displacement ( $y_0$  and  $y_1$ ) gives a second relationship with information about an integrated function of index along the ray path. Measurement of exit angle and displacement, two scalar quantities, does not provide enough information to determine the function  $n(y)$  along the ray path between  $y_0$  and  $y_1$  but could be used to evaluate two parameters of a local approximation to an index profile.

In the ray-optic approximation, mode conversion is like a distributed or convolved version of beam displacement. Instead of a ray, we now have an intensity distribution at each face of the slab,  $I_0(y)$ ,  $I_1(y)$ . For the axial case (the cylindrical case is more complicated due to off-axis rays from finite beam width and is beyond the scope of the current work), assuming the index of refraction and intensity distribution are continuous and smooth and that the incident beam has parallel rays,

$$I_1(y_0 + d(y_0)) = \frac{I_0(y_0)}{1 + \frac{\partial d}{\partial y_0}}, \quad (11)$$

where  $d(y_0) \equiv y_1 - y_0$  is the displacement of a ray and depends on the index distribution and the incidence angle. Eq. 11 becomes singular if there is a focal point at  $y_1$ . In this manner, intensity measurement is a proxy for displacement measurement, only making displacement measurement more complicated. But it may be that either the beams used are inherently wide compared with the measurement precision, meaning one could not escape making mode-shape measurements, or that due to precision differences in displacement measurement and intensity measurement there would still be an advantage to the latter. In any case, Eq. 11 could be useful to predict mode conversion effects based on displacement. Making multiple measurements per beam position (mode characteristics, displacement, and angular deflection), could allow some reduction in measurement driven errors. For normally incident Gaussian beams with small displacements (single parameter fit to index distribution over any given beam path), published calculations show detailed wave-optic predictions of mode conversion [6].

## A. Index Profile Computation

### 1. Deflection only method

It may be useful to reframe Eq. 9 in its analytically distilled form to understand how it might lead to computation of index profile. Eq. 9 evaluated at the exit side of the slab,

$$\frac{1 + y_1'^2}{1 + y_0'^2} = \frac{n_1^2}{n_0^2}, \quad (12)$$

has measured quantities on the left-hand side and values of the unknown index profile on the right-hand side. Taking the natural logarithm of both sides and calling

$$g(y_0) \equiv \ln \left( \frac{1 + y_1'^2}{1 + y_0'^2} \right)$$

and

$$\zeta(y) \equiv 2 \ln n(y),$$

yields

$$g(y_0) = \zeta(y_0 + d(y_0)) - \zeta(y_0). \quad (13)$$

Presuming that  $\frac{dy_1}{dy_0} > 0$  (which is satisfied if there is no ray crossing in the medium) and the index is known either along an interval  $[y_0, y_0 + d(y_0)]$  or at a point where  $\frac{dn}{dy} = 0$ , the index could be calculated everywhere (calculating each successive value of  $\zeta$  from previously known values, where which value in Eq. 13 would be previously known depends on the sign of  $d$ ). Eq. 13 could be approached analytically (see appendix A), but in practice the progressive sweep described here is more likely to be useful.

## 2. Displacement only and mixed methods

Equations 10 and 12, together with measurements of  $d$  and  $y_1'$ , form a basis for index determination. Because Eq. 10 is not analytically integrable for all  $n(y)$ , index profile estimation requires some numerical approximation. The approaches to approximating solutions to Eq. 10 can take the form of assuming properties, such as piecewise linearity, of the index profile or properties of the ray paths. These are joined by assumptions about small displacements relative to the index gradient or thin slabs.

**Approximation A:** For the special case where the incident ray is almost normal to the slab surface, it is useful to rewrite Eq. 10 as

$$t = \int_0^{d(y_0)} \frac{d\Delta y}{\sqrt{\left(\sqrt{1 + y_0'^2} \frac{n}{n_0} - 1\right) \left(\sqrt{1 + y_0'^2} \frac{n}{n_0} + 1\right)}}. \quad (14)$$

For  $\frac{(n-n_0)}{n_0} \equiv \tilde{n} \ll 1$  and  $y_0' \ll 1$ , Eq. 10 can be approximated by

$$t \approx \int_0^{d(y_0)} \frac{d\Delta y}{\sqrt{y_0'^2 + 2\tilde{n}}} . \quad (15)$$

**a. Approach 1: Linear Index over the Displacement of Any Given Ray**

If fractional index changes are small over length scales of the order of the slab thickness, rays deflect only a small amount and therefore traverse indices of the order of the index at the entry point. Assume the index profile encountered by any given ray can be well approximated by a linear function:

$$n(y) = an_0(y - y_0) + n_0 . \quad (16)$$

Plugging this form into Eq. 10 yields

$$t = \int_0^{d(y_0)} \frac{d\Delta y}{\sqrt{(1 + y_0'^2)(a^2\Delta y^2 + 2a\Delta y + 1) - 1}} . \quad (17)$$

Integration yields,<sup>1</sup>

$$\begin{aligned} & \left( 1 + \frac{y_0'}{\sqrt{1 + y_0'^2}} \right) e^{at\sqrt{1+y_0'^2}} \\ & = (1 + ad) + \sqrt{(1 + ad)^2 - \frac{1}{1 + y_0'^2}} , \end{aligned} \quad (18)$$

which cannot be solved explicitly but can readily be solved numerically for  $a$ . This would yield a piecewise linear solution to the index, which would in general not be precisely compliant with Eq. 12.

Eq. 17 can be reduced to Eq. 15 under the assumptions of Approximation A, noting that  $\tilde{n} = a\Delta y$  for this case, and then integrated and solved for the local index gradient

$$a = \frac{2}{t} \left( \frac{d}{t} - y_0' \right) . \quad (19)$$

As with Eq. 18, this over-constrains the independently measured ray exit slope (unless the true index profile is linear). Under these approximations of a linear index profile with small angle of incidence and small index change over the ray path, the ray path internal to the slab will be given by

---

<sup>1</sup> Wolfram's online Integrator Engine (<http://integrals.wolfram.com/index.jsp>).

$$y = \frac{1}{2}ax^2 + y'_0x + y_0,$$

so these approximations are equivalent to assuming parabolic ray paths as proposed by Barnard and Ahlborn [9].

### **b. Approach 2: Quadratic Index over the Displacement of Any Given Ray**

The quadratic approximation has the advantage that the number of unknown parameters matches the number of measurements.

$$n(y) = n_0a(y - y_0) + n_0b(y - y_0)^2 + n_0. \quad (20)$$

I am unaware of an explicit solution of Eq. 10 emerging from this form; however, under Approximation A (Eq. 15) with

$$\begin{aligned} \tilde{n} &= a\Delta y + b\Delta y^2, \\ t &= \int_0^{d(y_0)} \frac{d\Delta y}{\sqrt{y_0'^2 + 2(a\Delta y + b\Delta y^2)}}, \end{aligned} \quad (21)$$

which yields (Wolfram Integrator)

$$t\sqrt{2b} = \ln \frac{a + 2bd + \sqrt{2b}\sqrt{y_0'^2 + 2(ad + bd^2)}}{a + y_0'\sqrt{2b}}. \quad (22)$$

Eq. 22 could be solved numerically together with the Approximation A equivalent of Eq. 12,

$$y_1'^2 = y_0'^2 + 2(ad + bd^2). \quad (23)$$

### **c. Other Approximations**

While this type of approach could theoretically be extended to higher order polynomial approximations to the local index profile (representing Taylor series expansions), there would not be enough measurements to evaluate the parameters of such a framework. An alternative would be to look at different expansions of the local index profile, particularly those admitting explicit integration of Eq. 10. A one-parameter example of such would be an exponential profile, however, a two parameter alternative would allow the exit slope and displacement measurements to both be used without over-constraining the problem. Published work includes a list of explicitly integrable axial index distributions (e.g. [5]).

### 3. Refraction at Interfaces

This analysis has so far neglected the discrete refraction at the ray entrance and exit points. The slopes  $y'_0$  and  $y'_1$  referenced in all the preceding analysis represent the entrance and exit slopes just inside the slab boundary. Transformation into the measurable slopes just outside the slab boundary follows. The classic statement of Snell's law,

$$n_1 \sin \theta_1 = n_2 \sin \theta_2 ,$$

can be written in terms of slopes instead of angles. Adopting the notation that  $\hat{y}'_0$  and  $\hat{y}'_1$  represent the external slopes corresponding to the internal slopes  $y'_0$  and  $y'_1$ , and  $n_a$  represents the ambient index of refraction,

$$n_a \frac{\hat{y}'_i}{\sqrt{1 + \hat{y}'_i{}^2}} = n_i \frac{y'_i}{\sqrt{1 + y'_i{}^2}} , \quad (24)$$

where  $i$  is either 0 or 1. Combining Eqs. 24 and 12 leads to

$$n_1^2 = n_0^2 + n_a^2 \left( \frac{\hat{y}'_1{}^2}{1 + \hat{y}'_1{}^2} - \frac{\hat{y}'_0{}^2}{1 + \hat{y}'_0{}^2} \right) . \quad (25)$$

Eq. 25 is the corrected equivalent of the deflection relation Eq. 12. The corrected equivalent of Eq. 10, the displacement relation, is

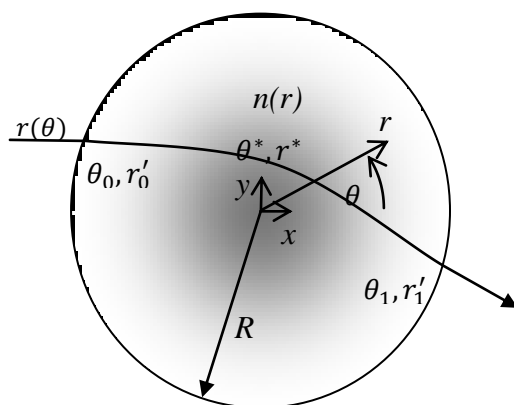
$$t = \int_{y_0}^{y_1} \frac{dy}{\sqrt{\left( \frac{1 + \hat{y}'_0{}^2}{n_0^2 + (n_0^2 - n_a^2)\hat{y}'_0{}^2} \right) n^2 - 1}} . \quad (26)$$

Note that for normal incidence, there is no refraction at the entrance surface.

## 4. Radial or Spherical Gradients

---

Due to symmetry, the rays in a planar circular slice through a radially symmetric cylinder will remain in the plane of the slice. In a concentric spherical medium, ray paths will all remain in the plane they share with the center of the sphere and they will be identical to those in a cylindrical medium with the same radial index dependence.



For this case, Eq. 1 reduces to

$$\frac{d \ln n}{dr} = \frac{r r'' - 2r'^2 - r^2}{r(r^2 + r'^2)}, \quad (27)$$

where primes indicate differentiation with respect to  $\theta$  along a ray. Integration of Eq. 27 yields

$$\frac{dr}{d\theta} = \pm \sqrt{\frac{n^2 r^4}{n_0^2 R^4} (R^2 + r_0'^2) - r^2}, \quad (28)$$

where  $R$  is the outer radius of the element,  $n_0$  is the index on the outer boundary, and  $r_0'$  is  $\left. \frac{dr}{d\theta} \right|_{r=R}$ . In dimensionless terms, letting

$$\hat{n} \equiv \frac{n}{n_a}, \quad \hat{r} \equiv \frac{r}{R},$$

where  $n_a$  is the ambient index of refraction,

$$\frac{d\hat{r}}{d\theta} = \pm \sqrt{\frac{\hat{n}^2 \hat{r}^4}{\hat{n}_0^2} (1 + \hat{r}_0'^2) - \hat{r}^2}. \quad (29)$$

Hence, for the radially symmetric medium as with the planar media, the local ray slope is dependent only on the boundary condition and the local index of refraction, not the intermediate path. The sign ambiguity emerges from the symmetry of the inbound and outbound paths in the medium.

Previous work on radially symmetric media limited investigation to azimuthally complete media such as fiber-optic preforms. For manufacture of spherical shell sections such as hemispherical lens components, exposed surfaces provide an opportunity to use the deflection technique embodied in Eq. 29 to directly measure the refractive index profiles.

For azimuthally complete media (full spheres or cylinders), the only accessible surface has a uniform index of refraction, and therefore nothing can be learned from the angle of the emerging beam relative to the surface (deflection). Displacement in the radial realm measures the difference in azimuth between the entry and exit points of the beam. To integrate Eq. 29 into the displacement relation, one must first identify the innermost transit point of the beam,  $\hat{r}^*$ , where symmetry dictates  $\frac{d\hat{r}}{d\theta} = 0$ . This satisfies the relation

$$r^* = \frac{\hat{n}_0}{\hat{n}^*} \frac{1}{\sqrt{1 + \hat{r}_0'^2}}, \quad (30)$$

where  $\hat{n}^*$  is the relative index at  $\hat{r}^*$ . In terms of angle of incidence  $\hat{\phi}$ , where the initial internal angle after refraction  $\phi$  is given by Snell's law,

$$\begin{aligned} \hat{n}_0 \sin \phi &= \sin \hat{\phi}, \\ \cot \phi &= \left. \frac{d\hat{r}}{d\theta} \right|_{\hat{r}=1}. \end{aligned}$$

In these terms, Eqs. 29 and 30 can be written as

$$\frac{1}{\hat{r}} \frac{d\hat{r}}{d\theta} = \pm \sqrt{\hat{n}^2 \hat{r}^2 \csc^2 \hat{\phi} - 1} \quad (31)$$

and

$$\hat{n}^* \hat{r}^* = \hat{n}_0 \sin \phi = \sin \hat{\phi}, \quad (32)$$

indicating that the behavior is scale invariant. The angle of the ray with the local gradient,  $\psi$ , is given by

$$\cot \psi = \frac{1}{\hat{r}} \frac{d\hat{r}}{d\theta}.$$

In terms of this angle, the invariant of Eq. 31 can be written as

$$\sin^2 \hat{\phi} = \hat{n}^2 \hat{r}^2 \sin^2 \psi, \quad (33)$$

equivalent to that in [10] or [1].

Integration of Eq. 31 from the outer boundary to  $\hat{r}^*$  and back yields

$$\Delta\theta = \pm 2 \int_{\hat{r}^*}^1 \frac{d\hat{r}}{\hat{r} \sqrt{\hat{n}^2 \hat{r}^2 \csc^2 \hat{\phi} - 1}}. \quad (34)$$

Index reconstruction proceeds as follows. Let

$$\xi(\hat{r}) \equiv \hat{n}(\hat{r})\hat{r}. \quad (35)$$

Suppose  $\xi(\hat{r})$  is a one-to-one mapping. Substitution of Eq. 35 into Eq. 34 yields

$$\Delta\theta(\hat{\phi}) = \pm 2 \sin \hat{\phi} \int_{\sin \hat{\phi}}^{\hat{n}_0} \frac{f'(\xi) d\xi}{\sqrt{\xi^2 - \sin^2 \hat{\phi}}}. \quad (36)$$

where

$$f(\xi) \equiv \ln \hat{r}(\xi). \quad (37)$$

In a practical scanning system, a beam parallel to the  $x$ -axis will be translated along the  $y$ -axis. Letting the position of the beam be

$$\hat{y} \equiv \frac{y}{R} = \sin \hat{\phi}, \quad (38)$$

and considering the negative instance of Eq. 36 (e.g. rays above the  $x$ -axis traveling in the positive  $x$ -direction), multiplication and integration in a manner similar to that of an Abel integral transform yields

$$\int_{\xi}^1 \frac{\Delta\theta(\hat{y}) d\hat{y}}{\sqrt{\hat{y}^2 - \xi^2}} = - \int_{\xi}^1 \int_{\hat{y}}^{\hat{n}_0} \frac{2\hat{y}f'(\tau)}{\sqrt{\hat{y}^2 - \xi^2} \sqrt{\tau^2 - \hat{y}}} d\tau d\hat{y}. \quad (39)$$

Switching the order of integration and presuming  $\hat{n}_0 > 1$ ,

$$\begin{aligned} - \int_{\xi}^1 \frac{\Delta\theta(\hat{y}) d\hat{y}}{\sqrt{\hat{y}^2 - \xi^2}} &= \int_{\xi}^1 \int_{\xi}^{\tau} \frac{2\hat{y}f'(\tau)}{\sqrt{\hat{y}^2 - \xi^2} \sqrt{\tau^2 - \hat{y}}} d\hat{y} d\tau + \int_1^{\hat{n}_0} \int_{\xi}^1 \frac{2\hat{y}f'(\tau)}{\sqrt{\hat{y}^2 - \xi^2} \sqrt{\tau^2 - \hat{y}}} d\hat{y} d\tau \\ &= \int_{\xi}^1 f'(\tau) \left[ -\tan^{-1} \left( \frac{\tau^2 + \xi^2 - 2\hat{y}^2}{2\sqrt{\hat{y}^2 - \xi^2} \sqrt{\tau^2 - \hat{y}}} \right) \right]_{\hat{y}=\xi}^{\tau} d\tau \\ &\quad + \int_1^{\hat{n}_0} f'(\tau) \left[ -\tan^{-1} \left( \frac{\tau^2 + \xi^2 - 2\hat{y}^2}{2\sqrt{\hat{y}^2 - \xi^2} \sqrt{\tau^2 - \hat{y}}} \right) \right]_{\hat{y}=\xi}^1 d\tau \end{aligned}$$

Applying the boundary condition  $f(\hat{n}_0) = 0$  and rearranging yields

$$f(\xi) = -\frac{1}{\pi} \int_{\xi}^1 \frac{\Delta\theta(\hat{y})d\hat{y}}{\sqrt{\hat{y}^2 - \xi^2}} - \frac{1}{2}f(1) + \frac{1}{\pi} \int_1^{\hat{n}_0} f'(\tau) \tan^{-1} \left( \frac{\tau^2 + \xi^2 - 2}{2\sqrt{1 - \xi^2}\sqrt{\tau^2 - 1}} \right) d\tau. \quad (40)$$

From Eqs. 32 and 38,

$$\xi^* \equiv \hat{n}^* \hat{r}^* = \hat{y}. \quad (41)$$

Eq. 41 indicates that from the tangential ray at  $\hat{y} = 1$  to the normal ray at  $\hat{y} = 0$  each ray penetrates progressively deeper into the medium so that reconstruction of the refractive index profile at position  $\xi = \hat{y}$  in Eq. 40 depends only on the measured displacement of rays corresponding to greater values of  $\hat{y}$ . However, finite surface refraction when the medium has an index of refraction greater than ambient prevents progressive interrogation up to the surface; from Eq. 32, even a ray tangent to the surface ( $\sin \hat{\phi} = 1$ ) penetrates to  $\xi = 1$ . Thus, for all incident rays, the effect of the medium from the boundary to  $\xi = 1$  manifests only in an aggregated fashion. As a result, unless the ambient index of refraction matches or exceeds the surface index of refraction, displacement results will not allow full reconstruction of the index profile.<sup>2</sup> For a medium immersed in index matched fluid, the last two terms in Eq. 40 vanish, and the full index profile can be reconstructed.

Returning to azimuthally incomplete media, which would allow beam exit from boundaries of varying refractive index (e.g. a lens cut from a spherically symmetric distribution or a hemisphere or hemispherical shell), Eq. 33 allows direct index reconstruction. If the boundary of the medium is along a radial line (normal to the iso-indicial surfaces), the external exit angle relative to the surface normal  $\hat{\alpha}$  gives the following relationship for deriving the index at the exit point:

$$\hat{n} = \sqrt{\sin^2 \hat{\alpha} + \frac{\sin^2 \hat{\phi}}{\hat{r}^2}}. \quad (42)$$

This would allow the nondestructive evaluation by the deflection method of hemispherical lens preforms or the like.

Mode conversion for the spherical case is more complicated because finite beam width leads to rays in different planes of refractive index symmetry. Treatment of such is beyond the scope of this work.

---

<sup>2</sup> For the lens design problem that is the inverse of the metrology problem described herein (given a set of desired ray displacements, what index would be needed), Eq. 40 implies that the refractive index profile from the boundary to  $\xi = 1$  could be chosen arbitrarily, and the profile from  $\xi = 1$  to the center would follow.

## 5. Conclusion

---

For media with axial, cylindrical, or spherical distributions of refractive index, a ray slope invariant (Eqs. 3, 9, and 33) allows the use of ray deflection as a means of measuring the index of refraction at the exit point as a function of the index of refraction at the entrance. This is only useful when surfaces of varying index are exposed, in which case approximate reconstructions of the index profile are possible with a finite number of measurements. Ray displacement and beam mode conversion also capture information about the index distribution and can be used to reconstruct or help reconstruct the index distribution. For azimuthally complete spherical gradients or radial gradients viewed normal to the axis of symmetry, index reconstruction is only possible in an index-matching fluid. For the other cases considered, numerical approaches are required, but index reconstruction is possible. The analysis here provides a survey of the derivations and proposed solution methods for these approaches with an eye toward metrology applications for gradient index lens manufacture.

## Appendix A

### Solution to beam deflection angle method

---

Beginning with Eq. 13, the general problem consists of finding  $\zeta(y)$  satisfying

$$\zeta(y + d(y)) - \zeta(y) = g(y), \quad (\text{A1})$$

given  $g(y)$  and  $d(y)$ . Eq. A1 is like a continuous version of a difference equation. In that vein, the solution can be separated into a homogeneous and a particular solution,

$$\zeta(y) = \zeta_h(y) + \zeta_p(y),$$

where the homogeneous solution satisfies

$$\zeta_h(y + d(y)) - \zeta_h(y) = 0. \quad (\text{A2})$$

Suppose there are two solutions to Eq. A1,  $\zeta_1(y)$  and  $\zeta_2(y)$ . Taking the difference between the two versions of Eq. A1, one with each solution plugged in,

$$\Delta\zeta(y + d(y)) - \Delta\zeta(y) = 0,$$

where  $\Delta\zeta(y) \equiv \zeta_1(y) - \zeta_2(y)$ . Thus, any solutions to Eq. A1 differ by a homogeneous solution. Therefore, finding any particular solution and adding it to the general homogeneous solution will provide a complete solution to Eq. A1. By inspection, the general solution to Eq. A2 (guaranteeing only continuity) is any periodic function transformed over successive periods by the known function  $d(y)$  as long as  $\frac{d}{dy}(y + d(y)) > 0$ . Let  $h(y) \equiv y + d(y)$ . Taking an arbitrary starting point  $y_a$ , and defining an arbitrary periodic function  $\phi(y)$  over  $[y_a, y_a + d(y_a)]$ ,

$$\zeta_h = \begin{cases} \phi(y) & y_a \leq y < h(y_a) \\ \phi(h^{-1}(y)) & h(y_a) \leq y < h(h(y_a)) \\ \phi(h^{-1}(h^{-1}(y))) & \vdots \\ \vdots & \vdots \end{cases}. \quad (\text{A3})$$

Because of the degrees of freedom inherent in the arbitrary periodic function, the boundary condition necessary to uniquely determine a solution must define the value of  $\zeta(y)$  over a full interval  $[y_a, y_a + d(y_a)]$ . Such a boundary condition would reduce the solution of Eq. A1 immediately to a recursive form like Eq. A3.

A particular solution can be identified using a Green's function approach. Let

$$u(h(y), \tilde{y}) - u(y, \tilde{y}) = \delta(y - \tilde{y}), \quad (\text{A4})$$

where  $\delta(y)$  is the Dirac delta function. Let

$$h^n(y) \equiv \underbrace{h\left(h\left(h\left(\dots h(y) \dots\right)\right)\right)}_{n \text{ nested compositions}}$$

and likewise for  $h^{-n}(y)$  as  $n$  nested compositions of  $h^{-1}(y)$ . Two particular solutions to Eq. A4, differing, as required, by a function of the form of Eq. A3, are

$$u(y, \tilde{y}) = \sum_{n=1}^{\infty} \pm \delta(h^{\mp n}(y) - \tilde{y}) \quad (\text{A5})$$

both of which are forms of Dirac combs (picket fence) on a half space.

To construct  $\zeta_p(y)$ , integrate Eq. A4 times the right-hand side of Eq. A1,

$$\begin{aligned} \int_{-\infty}^{\infty} g(\tilde{y})(u(h(y), \tilde{y}) - u(y, \tilde{y}))d\tilde{y} &= \int_{-\infty}^{\infty} g(\tilde{y})\delta(y - \tilde{y})d\tilde{y} \\ &= g(y). \end{aligned} \quad (\text{A6})$$

Comparing the terms of Eqs. A7 and A1 reveals that

$$\zeta_p(y) = \int_{-\infty}^{\infty} g(\tilde{y})u(y, \tilde{y})d\tilde{y}. \quad (\text{A7})$$

Taking the Green's function from Eq. A5,

$$\begin{aligned} \zeta_p(y) &= \int_{-\infty}^{\infty} g(\tilde{y}) \sum_{n=1}^{\infty} \pm \delta(h^{\mp n}(y) - \tilde{y}) d\tilde{y} \\ &= \pm \sum_{n=1}^{\infty} g(h^{\mp n}(y)). \end{aligned} \quad (\text{A8})$$

If either  $g(h^n(y))$  or  $g(h^{-n}(y))$  is appropriately convergent, then a solution has been identified. If, as may often be the case, on at least one end of the slab the index becomes homogeneous, then

$$\lim_{n \rightarrow \infty} g(h^{\pm n}(y)) = 0, \quad (\text{A9})$$

and convergence of Eq. A9 or A10 is possible. The index profile follows from

$$n(y) = e^{\zeta(y)/2}. \quad (\text{A10})$$

The solution method above guarantees that, for smooth  $\phi(y)$ ,  $\zeta(y)$  will be at least as smooth as  $g(y)$  within each interval  $[h^n(y_a), h^{n+1}(y_a)]$ . Guaranteeing smoothness across the interval boundaries would further constrain the solution.

## References

---

- [1] E. W. Marchand, *Gradient Index Optics*, New York: Academic Press, 1978.
- [2] O. Wiener, "Darstellung gekrummter Lichtstrahlen und Verwerthung derselben zur Untersuchung von Diffusion und Wärmeleitung," *Annalen der Physik*, vol. 285, no. 5, pp. 105-149, 1893.
- [3] G. Beliakov and D. Y. C. Chan, "Analysis of inhomogeneous optical systems by the use of ray tracing. I. Planar systems," *Applied Optics*, vol. 36, no. 22, pp. 5303-5309, 1997.
- [4] G. Beliakov and D. Y. C. Chan, "Analysis of inhomogeneous optical systems by the use of ray tracing. II. Three-dimensional systems with symmetry," *Applied Optics*, vol. 37, no. 22, pp. 5106-5111, 1998.
- [5] G. Beliakov and S. Buckley, "Reconstruction of the refractive index profile of planar waveguides using ray tracing analysis," in *Optical networking : technologies, traffic engineering and management : conference proceedings*, Melbourne, Australia, 2003.
- [6] A. Mandelis and B. S. H. Royce, "Fundamental-mode laser-beam propagation in optically inhomogeneous electrochemical media with chemical species concentration gradients," *Applied Optics*, vol. 23, no. 17, pp. 2892-2901, 1984.
- [7] P. L. Chu, "Nondestructive Measurement of Index Profile of an Optical-Fibre Preform," *Electronics Letters*, vol. 13, no. 24, pp. 736-738, 1977.
- [8] A. D. Polyanin, *Handbook of Integral Equations*, Washington, D.C.: CRC Press, 1998.
- [9] A. J. Barnard and B. Ahlborn, "Measurement of refractive index gradients by deflection of a laser beam," *American Journal of Physics*, vol. 43, no. 7, pp. 573-574, 1975.
- [10] R. K. Luneburg, *Mathematical Theory of Optics*, Berkeley: University of California Press, 1964.
- [11] A. Sharma, D. V. Kumar and A. K. Ghatak, "Tracing rays through graded-index media: a new method," *Applied Optics*, vol. 21, no. 6, pp. 984-987, 1982.

**REPORT DOCUMENTATION PAGE***Form Approved*  
OMB No. 0704-0188

Public reporting burden for this collection of information is estimated to average 1 hour per response, including the time for reviewing instructions, searching existing data sources, gathering and maintaining the data needed, and completing and reviewing this collection of information. Send comments regarding this burden estimate or any other aspect of this collection of information, including suggestions for reducing this burden to Department of Defense, Washington Headquarters Services, Directorate for Information Operations and Reports (0704-0188), 1215 Jefferson Davis Highway, Suite 1204, Arlington, VA 22202-4302. Respondents should be aware that notwithstanding any other provision of law, no person shall be subject to any penalty for failing to comply with a collection of information if it does not display a currently valid OMB control number. **PLEASE DO NOT RETURN YOUR FORM TO THE ABOVE ADDRESS.**

1. REPORT DATE March 2013		2. REPORT TYPE Final		3. DATES COVERED (From-To) November 2012 – February 2013	
4. TITLE AND SUBTITLE  Measurement of Gradient Index Materials by Berm Deflection, Displacement, or Mode Conversion (Journal Version)				5a. CONTRACT NUMBER W91WAW-09-C-0003	
				5b. GRANT NUMBER	
				5c. PROGRAM ELEMENT NUMBER	
6. AUTHOR(S)  Jeremy Teichman				5d. PROJECT NUMBER	
				5e. TASK NUMBER DA-2-3226	
				5f. WORK UNIT NUMBER	
7. PERFORMING ORGANIZATION NAME(S) AND ADDRESS(ES)  Institute for Defense Analyses 4850 Mark Center Drive Alexandria, VA 22311-1882				8. PERFORMING ORGANIZATION REPORT NUMBER  IDA Paper NS P-4994 Log: H13-000324	
9. SPONSORING/MONITORING AGENCY NAME(S) AND ADDRESS(ES)  Defense Advanced Research Projects Agency 675 North Randolph Street Arlington, VA 22203-2114				10. SPONSOR/MONITOR'S ACRONYM(S) DARPA	
				11. SPONSOR/MONITOR'S REPORT NUMBER(S)	
12. DISTRIBUTION/AVAILABILITY STATEMENT  Approved for public release; distribution is unlimited. (24 April 2013)					
13. SUPPLEMENTARY NOTES					
14. ABSTRACT  For media with heterogeneous index of refraction, rays follow curved paths. This paper describes methods exploiting knowledge of the relationship between refractive index distribution and ray paths to estimate the refractive index distribution based on laser beam deflection, displacement, and mode conversion on passage through the media. The work covers axial, radial (cylindrical), and spherical refractive index distributions.					
15. SUBJECT TERMS  Gradient Index Optics, Refraction, Optical Measurement, Beam Deflection, Metrology, Index of Refraction, Non-destructive evaluation					
16. SECURITY CLASSIFICATION OF:			17. LIMITATION OF ABSTRACT  SAR	18. NUMBER OF PAGES  22	19a. NAME OF RESPONSIBLE PERSON Brian Holloway
a. REPORT Uncl.	b. ABSTRACT Uncl.	c. THIS PAGE Uncl.			19b. TELEPHONE NUMBER (include area code) 703-526-4064